

Fitness Landscape Analysis and Optimization of Coupled Oscillators

David Newth*

Markus Brede†

*CSIRO Centre for Complex Systems Science,
G.P.O. Box 284,
Canberra, ACT 2601, Australia*

Synchronization in chaotic oscillatory systems has a wide array of applications in biology, physics, and communications systems. Over the past 10 years there has been considerable interest in the synchronization properties of small-world and scale-free networks. In this paper, we define the fitness of a configuration of coupled oscillators as its ability to synchronize, which is related to the ratio of the largest and smallest eigenvalues of the coupling matrix. After an analysis of the fitness landscape of the coupled oscillators problem, we employ an optimization algorithm to determine network structures that lead to an enhanced ability to synchronize. The optimized networks generally have low clustering, small diameters, short path-length, are disassortative, and have a high degree of homogeneity in their degree and load distributions.

1. Introduction

Over the past 10 years, it has been shown that many natural and man-made systems share common features in the way their underlying components are arranged [1, 2]. A recurring theme in much of this research is the notion that the network topology must have some bearing on the dynamics taking place upon the network [3, 4]. One common emergent feature of many coupled oscillatory systems is for the dynamics to self-organize into a rhythmical beat. Such behavior has been observed in populations of fire flies, the heart, sets of coupled lasers, and even the brain [5].

The synchronization of networks of coupled oscillators, in particular synchronization on small-world and scale-free networks, has been widely studied over the past five years [2, 3, 5, 6–9]. While investigating how the topological properties of certain model networks affect synchronization, several studies have found somewhat conflicting results. For example Hong *et al.* [6] found that increasing degree heterogeneity

*Electronic mail address: david.newth@csiro.au.

†Electronic mail address: markus.brede@csiro.au.

promoted synchronizability, while Nishikawa *et al.* [7] observed the opposite effect. In this paper we take a different approach. Instead of investigating the synchronizability properties of given classes of networks, we let networks evolve towards a configuration that exhibits superior synchronizability. More precisely, we adopt the framework outlined in [10] to determine the stability of the synchronized state of a set of oscillators coupled by a network. In the remainder of this paper this measure defines a network's fitness. To choose an appropriate optimization scheme an understanding of the structure of the fitness landscape over the space of all network configurations is essential.

The aim of the paper is twofold. First we characterize the structure and complexity of the fitness landscape of the coupled oscillators problem. We are particularly interested in how the landscape changes with the number of oscillators. Based thereon, we develop a stochastic optimization scheme and generate ensembles of networks with superior synchronization properties. Second we analyze topological features of these networks and identify network characteristics that lead to enhanced synchronizability.

The organization of the paper is as follows. In section 2 we outline the general model used to describe a network of coupled oscillators. We give a brief summary of the framework of Pecora and Carroll [10] for characterizing the synchronizability of a network of coupled oscillators. Section 3 describes the notion of a fitness landscape and introduces the information theoretic measures we use to characterize the structure of the fitness landscape. We proceed by studying the fitness landscape of the oscillator problem and develop an optimization scheme which is discussed in section 4. After presenting an analysis of topological properties of optimal network configurations, section 5 concludes with a summary and a discussion of possible implications of our results.

2. Coupled oscillators

The tendency for a system's dynamics to self-organize into a rhythmic beat has been studied in fields as diverse as mathematics, biology, neuroscience, electrical engineering, and laser physics (see [8, 9, 11] for overviews). Over the past decade studies of coupled oscillators have shown that certain network properties can enhance or diminish a system's ability to synchronize. Here we follow the framework of Pecora and Carroll [10] for determining synchronizability. We consider a system of N coupled oscillators. Let x_i be the m -dimensional vector of state variables of node i . The dynamics of the coupled oscillators are governed by:

$$\dot{x}_i = F(x_i) + \sigma \sum_j G_{ij} H(x_j), \quad (1)$$

where $F(\cdot)$ determines the dynamics of the individual oscillators without coupling, while $H(\cdot)$ and the matrix G describe the interactions between them. The coupling matrix G is constructed as:

$$g_{ij} = \begin{cases} -1 & \text{if } i \text{ is connected to } j, i \neq j \\ 0 & \text{if } i \text{ is not connected to } j, i \neq j, \\ k_i & \text{if } i = j \end{cases} \quad (2)$$

which ensures the existence of an invariant synchronization manifold. We only consider symmetric connections, which guarantees that all the eigenvalues of G are real. Let the eigenvalues of G be labeled $\lambda_N \geq \lambda_{N-1} \geq \dots \geq \lambda_2 \geq \lambda_1 = 0$. If G is connected then $\lambda_2 \neq 0$. The stability of the synchronized state $x_1 = x_2 = \dots = x_N$ is determined by the jacobian of the functions F and H , and the eigenvalues of G [10]. For a wide array of systems the synchronized state is linearly stable if all except the zero eigenvalue lie in a single parameter interval (α_1, α_2) , which is determined by the functions F and H . Independent of the actual system specifications, the ratio $r = \lambda_N/\lambda_2$ is an indicator of the synchronizability of the coupling scheme G . Small ratios imply good synchronizability. In the remainder of this paper the negative ratio $-r$ defines a network's fitness.

3. Fitness landscapes

The notion of a fitness landscape was first proposed by Sewell Wright [12] and serves as a powerful tool for visualizing the changes in the fitness of a population of individuals as they are guided *via* an evolutionary process. Although fitness landscapes were initially introduced as a non-mathematical tool for visualizing biological processes they have become an important aspect in optimization, search, and machine learning [13].

The performance of a search algorithm is intimately linked to the structure of the fitness landscape of the underlying problem. The complexity of a fitness landscape can be characterized by two properties: (1) epistasis (the degree to which each of the free parameters are dependent upon each other); and (2) modality (the number and arrangement of optima). While there have been a number of fitness landscape analysis techniques developed (e.g., [14]), we will only focus on the information theoretic framework proposed by Vassilev *et al.* in [15] where they outline four measures to characterize the structure of a fitness landscape. These are: (1) information content $H(\varepsilon)$ (an indication of the ruggedness of the landscape), (2) partial information content $M(\varepsilon)$ (an indication of the modality of the landscape), (3) information stability ε^* (an indication of the magnitude of the landscape's optima), and (4) density-basin information $b(\varepsilon)$ (an indication of the structure of the landscape around the optima).

We construct a sequence of fitness values $\{f_t\}_{t=0}^n$ obtained from a random walk upon the fitness landscape \mathcal{L} . This sequence contains

structural information about the landscape (it's epistasis and modality). In order to gain an understanding of the structure of the underlying fitness landscape we need to decompose $\{f_t\}_{t=0}^n$ into an ensemble of objects that describe the coarse-grained structure of the landscape. For this purpose we define $S(\varepsilon) = s_1, s_2, \dots, s_n$ to be a string of symbols where $s_i \in \{\bar{1}, 0, 1\}$. $S(\varepsilon)$ is obtained from $\{f_t\}_{t=0}^n$ by $s_i = \Psi_{f_i}(i, \varepsilon)$, where

$$\Psi_{f_i}(i, \varepsilon) = \begin{cases} \bar{1} & \text{if } f_i - f_{i-1} < -\varepsilon \\ 0 & \text{if } |f_i - f_{i-1}| \leq \varepsilon \\ 1 & \text{if } f_i - f_{i-1} > \varepsilon \end{cases} . \quad (3)$$

The parameter ε acts as a filter smoothing the fitness landscape. When $\varepsilon = 0$ minor changes in the landscape are detected. As ε is increased small-scale structures are removed, leaving only the major features of the landscape.

■ 3.1 Information theoretic measures

An entropic measure of subblocks within $S(\varepsilon)$ can be defined as:

$$H(\varepsilon) = - \sum_{p \neq q} P_{|pq|} \log_6 P_{|pq|}, \quad (4)$$

where $P_{|pq|}$ is the probability of the occurrence of the substring pq within $S(\varepsilon)$. This measure is an estimation of the ruggedness of the fitness landscape based on the diversity of the number of shapes encountered during a random walk. Another feature of fitness landscapes related to ruggedness is modality. The modality of the fitness landscape can be measured through the partial information content of $S(\varepsilon)$. The partial information content $M(\varepsilon)$ is obtained by removing all nonessential (repeated) substrings within $S(\varepsilon)$. We then define $M(\varepsilon)$ to be:

$$M(\varepsilon) = \frac{\mu}{n}, \quad (5)$$

where μ is the length of the compressed string $S'(\varepsilon)$ and n is the length of $S(\varepsilon)$.

The information content and partial information content characterize the diversity of structures found in $S(\varepsilon)$. As mentioned earlier ε acts as a filter through which the fitness landscape is observed. Information stability ε^* is the smallest ε value for which the fitness landscape becomes completely flat. That is, the string $S(\varepsilon^*)$ contains only zeros. Information stability serves as a measure of the magnitude of the changes in fitness encountered during the walk.

To characterize the structure of the fitness landscape around the optima, it is useful to study the diversity of flat and smooth structures upon the landscape. To do this we are only concerned with the sub-

strings: 00, 11, $\bar{1}\bar{1}$. The entropy of the distribution of these objects is then calculated as:

$$h(\varepsilon) = - \sum_{p \in \{1, 0, 1\}} P_{pp} \log_3 P_{pp}, \quad (6)$$

we will refer to this measure as the *density-basin information*.

3.2 Fitness landscape characteristics

The information theoretic measures outlined allow the inference of structural characteristics of a fitness landscape from a sequence of moves from a random walk on it [15]. We are particularly interested in the changes that occur to the fitness landscape as the problem scales (i.e., the number of nodes increases).

For this purpose we constructed time series data for random walks containing 300,000 moves. Regardless of the network configuration (i.e., number of nodes and edges) the information theory statistics appear to be stable. At each time step the fitness (r) of the current network configuration is calculated. A move between configurations consists of the random reassignment of an edge. This samples the space of all networks with N nodes and L edges. Time series data were compiled for systems containing 100, 150, 200, 250, 300, 350, 400, 450, and 500 nodes. The connectivity of each system was fixed to 0.1 which ensures the networks are above the connectivity threshold [16]. In all cases $\varepsilon = 0$, so that the fine detail of the landscape is exposed.

Figure 1 depicts changes in the characteristics of the fitness landscape as the number of oscillators increases. Figure 1(a) shows that as the system size increases the diversity of objects decreases. This means that the landscape becomes less rugged with increasing system size. The partial information content Figure 1(b) illustrates that as system size increases, smooth regions become larger. These two results suggest that as the number of oscillators grows, no new optima appear on the landscape. Instead the existing optima are becoming more rounded, move away from each other, and smooth regions separate the optima. The information stability (see Figure 1(c)) shows that as the system scales with size the difference in fitness values between any two adjacent configurations is reduced. This is another indicator that the fitness landscape is becoming smoother. In other words the degree of interdependence (epistasis) between the free parameters (in this case the individual edge assignments) is decreasing with size. Finally the density-basin information (Figure 1(d)) indicates that the area around the optima becomes smoother and more rounded as the number of oscillators grows. Combining these observations about the information stability and density-basin information, one realizes that once in the basin of attraction of an optimum it should be quite easy to discover it.

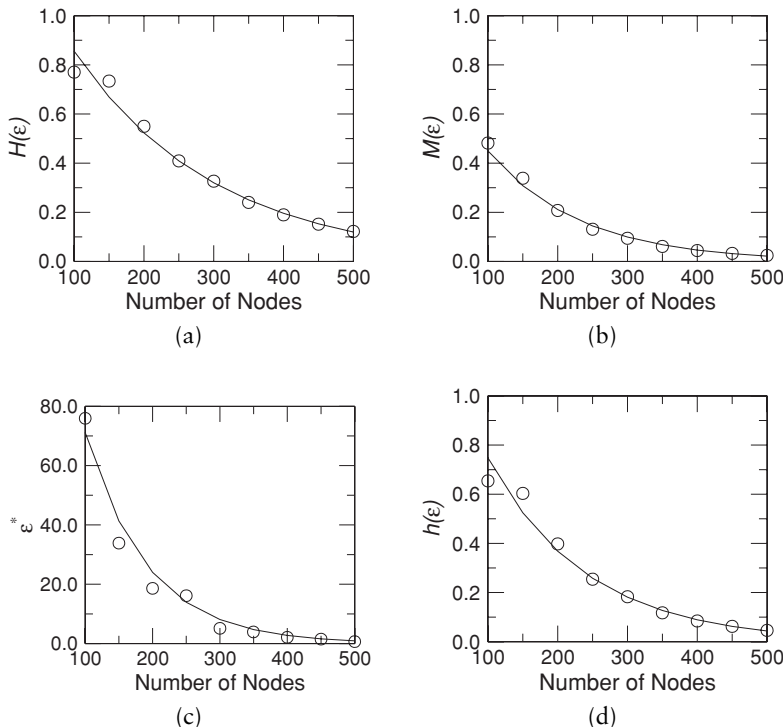


Figure 1. Fitness landscape characteristics as a function of system size. (a) Information content of the fitness landscape ($H(\varepsilon)$). As the system size increases, the ruggedness of the landscape decreases. (b) Partial information content ($M(\varepsilon)$). As the size of the system increases the fitness landscape becomes more modal. (c) Information stability (ε^*). During the walk the chance of encountering large optima decreases. (d) Density-basin information ($h(\varepsilon)$). As the number of nodes within the system increases, the structures around the optima become less diverse. Lines are for visual guidance only.

4. Optimization of coupled oscillators

To create networks with enhanced synchronizability we make use of the basic optimization scheme known as a stochastic hill-climber. The networks contain 500 nodes, and a fixed number of edges. The aim is to discover the optimal arrangement of the available edges that produces the highest degree of synchronizability. The basic optimization scheme consists of two stages. First, a small modification to the network is suggested. Essentially an edge is deleted from the network and inserted between two nodes that were not previously connected. Second, if the network is still connected, and is found to have an improved fitness,

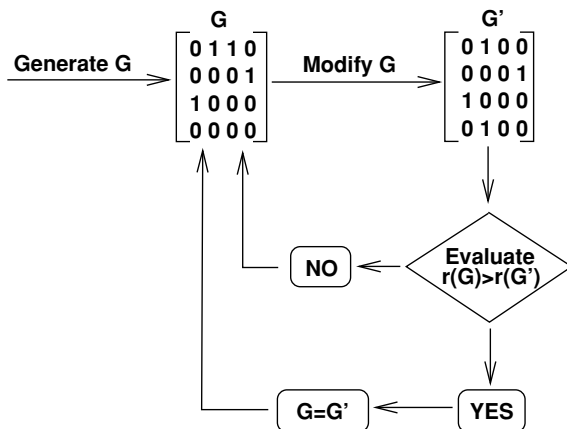


Figure 2. Setup of the stochastic hill-climber. Initially, the hill-climber is seeded with a network G that is to be optimized. At each time step, a random modification to G is suggested (G'). The fitness value of G' is calculated. Should $r(G') < r(G)$, G is replaced by G' , and the loop continues. This procedure is iterated until there is no improvement found after Δt time steps.

the suggested rewiring is accepted, otherwise it is rejected. These two steps are then repeated until no improvements are found during $\Delta t = N(N - 1)/2$ (such that every edge has on average been probed once) optimization steps.

Figure 2 visualizes this basic configuration of the stochastic hill-climber. The selection of this optimization scheme over others was straightforward. The analysis presented in section 3.2 demonstrated that as system size increases the fitness landscape becomes smoother, the optima become more rounded, whilst being separated by smooth regions. This allows us to suppose that most improvements made by the stochastic hill-climber will move the network toward the optimal topology. This means we do not need to find the best move at any given time step.

Another point to note is that the local neighborhood of any arbitrary point on the fitness landscape has $L(N(N - 1)/2 - L + 1)$ neighbors. For a system with (say) 100 nodes and 495 links the local neighborhood contains approximately 2×10^6 elements, and—for fixed connectivity C , that is, $L \sim CN(N - 1)/2$ —grows as $O(n^4)$. The use of a deterministic optimization routine would require the enumeration of the entire neighborhood, which is computationally intractable. Finally, we also explored the use of a genetic algorithm. However the population quickly converged, making mutation the sole search operator. So the search degrades to a stochastic hill-climber.

4.1 Network properties

To explore the topological properties of the optimized networks, we investigate a number of statistical characteristics that are commonly used to describe complex networks. The first statistic of interest is the diameter. The diameter of the network is the longest shortest path between two nodes within a network

$$D = \max l_{\min}(i, j), \quad (7)$$

where $l_{\min}(i, j)$, is the shortest path-length between nodes i and j . The average shortest path-length \bar{l} of a network is:

$$\bar{l} = \frac{2}{N(N - 1)} \sum_{i=1}^N \sum_{j=1}^N l_{\min}(i, j). \quad (8)$$

The next statistic we are concerned with is the degree of clustering found within the network. Clustering is commonly measured *via* the clustering coefficient C . Given a node i , with k_i neighbors, E_i is defined as the number of links that exist between the k_i neighbors. The clustering coefficient is the ratio between the number of links that exist between the neighbors E_i and the potential number of links $k_i(k_i - 1)/2$. Averaged across all nodes within the network the clustering coefficient is defined as:

$$C = \frac{1}{N} \sum_{i=1}^N \frac{E_i}{k_i(k_i - 1)}. \quad (9)$$

The combination of high clustering and small average shortest path-length are known as the small-world properties [17].

Another useful measure that has provided insight into the organization of complex networks is the degree of assortative mixing. A network is said to show assortative mixing if nodes of high degree are typically connected to other nodes of high degree. Conversely, in a dissassortatively mixed network nodes with many links tend to be adjacent to nodes with few neighbors. Following [18] we use a Pearson correlation coefficient α to quantify the assortativeness of a network. In [18] Newman defines this correlation as:

$$\alpha = \frac{c \sum_i j_i k_i - \left[c \sum_i \frac{1}{2} (j_i + k_i) \right]^2}{c \sum_i \frac{1}{2} (j_i^2 + k_i^2) - \left[c \sum_i \frac{1}{2} (j_i + k_i) \right]^2}, \quad (10)$$

where j_i and k_i are the degrees of the vertices at the ends of edge i , and all sums run over the L edges of the network. For a network with L edges we set $c = 1/L$. A network displays assortative mixing when $\alpha > 0$ and dissassortative mixing when $\alpha < 0$. While some social networks are assortative, many other networks with power law degree distributions are dissassortatively mixed [18].

It has also been shown that synchronizability is related to the betweenness centrality or the load on a vertex [7]. The load B_ν on a vertex ν is defined as [19]:

$$B_\nu = \frac{2}{(N-1)(N-2)} \sum_{i=1}^N \sum_{\substack{j=1 \\ j \neq i}}^N d_{ij}^\nu, \quad (11)$$

where $d_{ij}^\nu = 1$ if the shortest path between i and j passes through vertex ν and $d_{ij}^\nu = 0$ otherwise. To get an understanding of how loads are distributed across nodes we calculate the maximum vertex load B_{\max} , the average load B , and the standard deviation of the distribution across the entire network σ_B .

■ 4.2 Results

As an initial study, we seed our algorithm with three different initial conditions. We consider Erdős and Rényi random graphs, scale-free networks, and hypercubes of up to $N = 500$ nodes. Qualitative results do not depend upon system size. Each of the systems possess properties thought to promote synchronizability. For each class of networks, we ran the stochastic hill-climber 100 times for 10,000 optimization steps. Figure 3 shows the time evolution of $\langle r \rangle$ for the three configura-

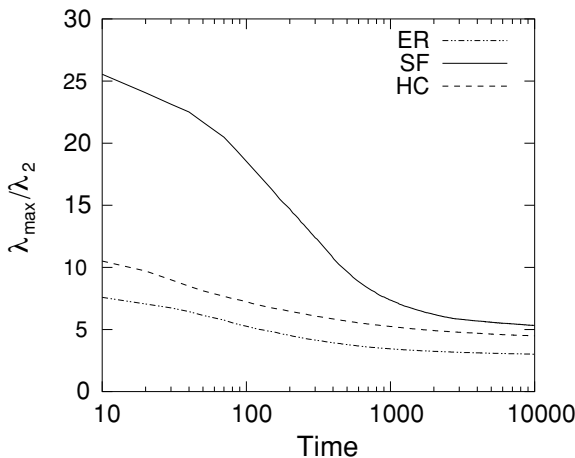


Figure 3. Time evolution during evolution averaged over an ensemble of scale-free networks (solid line), a hypercube (dashed line), and an ensemble of Erdős–Rényi random graphs (dotted line) with the same average number of links and size $N = 128$. The curves represent averages over different optimizations, each time starting with a different member of the ensemble (for Erdős–Rényi random graphs and scale-free networks). Because hypercubes represent local optima in network space, an annealing scheme was used in this case.

tions. It can be seen from this figure that after approximately 1,000 time steps there is no major improvement in r . Although the networks have the same (average) number of links, the final configurations still differ in their final average ratio $\langle r \rangle$. That is, the optimized networks obtained from scale-free and hypercube starting conditions represent suboptimal solutions within the landscape of all possible networks. The search algorithm created networks with better synchronization properties, when seeded with a random network. In the remainder of this paper we will only examine the changes in network topology where the starting condition was an Erdős and Rényi random graph. For the interested reader Brede and Newth [20] provide a systematic analysis of changes in other network types as they evolve.

We now focus on the statistical measures outlined in section 4.1. These measures provide a systematic framework for identifying topological properties associated with improved synchronizability. Many of the network properties can be directly attributed to their degree distribution. Figure 4 illustrates how the degree distribution changes as the networks approach the optima. Starting from the typical poissonian degree distribution of an Erdős–Rényi random graph at $t = 0$, we can see that as the network becomes “more optimized” the variance in the degree distribution collapses, and the distribution becomes heavily

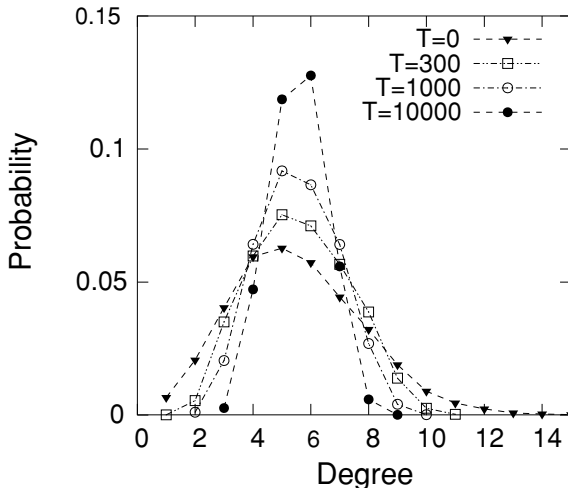


Figure 4. Evolution of the degree distribution. Initially the degree distribution conforms to that of an Erdős–Rényi random graph ($T = 0$). However as the synchronization properties are enhanced, the variance in the degree distribution collapses. Finally the degree distribution becomes very narrow and highly peaked around the average degree ($T = 10,000$). This suggests that the network is almost regular.

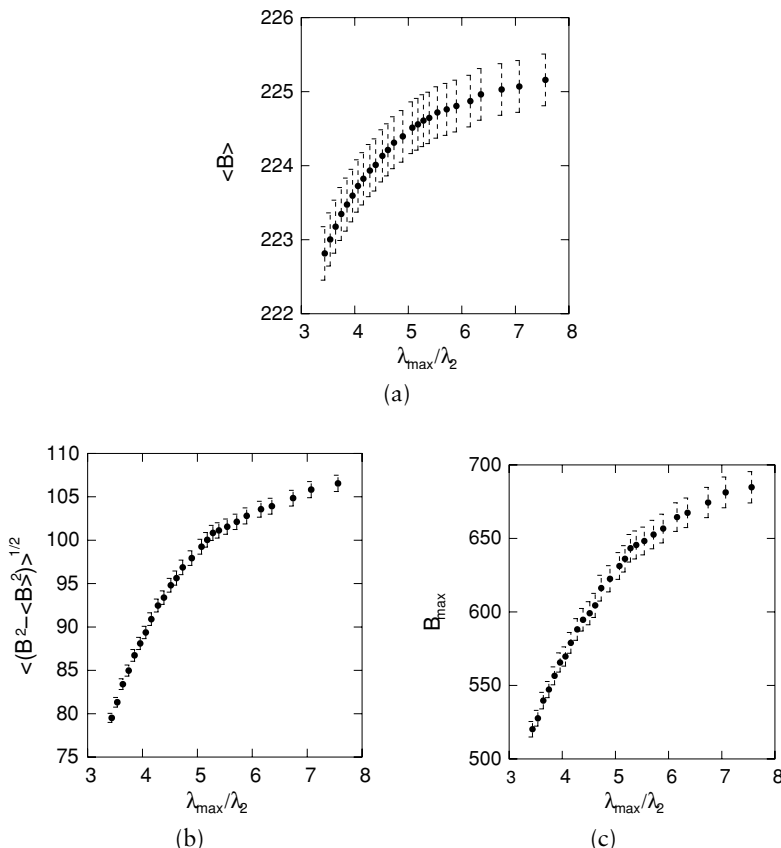


Figure 5. (a) Dependence of the loads on the eigenvalue ratio, (b) standard deviation of the load, and (c) maximum load. As can be seen in these plots, increased synchronizability is associated with lower maximum and average loads. This shows that synchronizability improves as the distribution of loads becomes more homogeneous.

peaked around the average degree $\langle k \rangle \approx 5$ ($t = 10,000$). This suggests that the network is becoming more regular, that is, every node has approximately the same number of edges.

The aforementioned regularities directly related to how load affects synchronizability (see Figure 5). We find that improved synchronizability is associated with a homogenous load distribution (small average load $\langle B \rangle$ and small variance σ_B), and reduced maximum load distribution (B_{\max}). This indicates that the flow of information between nodes within the network needs to be homogenous in order to maximize stability of the synchronized state. This clearly shows that hubs in scale-free networks may impede synchronization, as hubs tend to carry a high load.

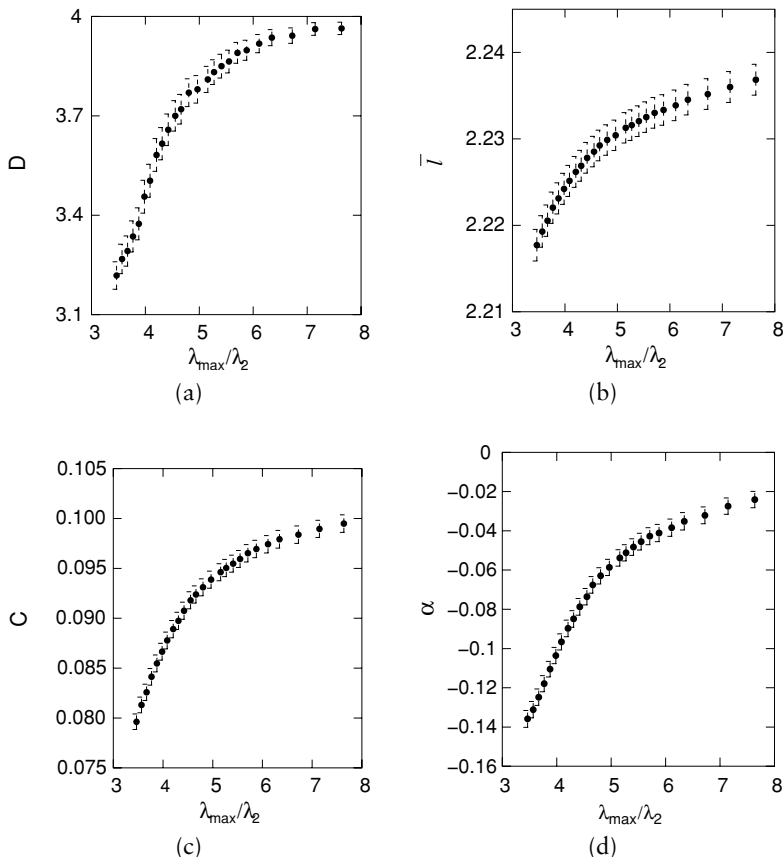


Figure 6. Evolution of various network statistics as a function of λ_{\max}/λ_2 . (a) Network diameter: As the diameter of the network increases the stability of the stable synchronized state decreases. (b) Average shortest path-length: Networks that have enhanced stability properties tend to have on average shorter path-lengths between nodes. (c) Clustering coefficient: Networks with enhanced synchronizability properties tend to have reduced clustering than those with reduced synchronizability. Locally these networks are very tree-like. (d) Assortativity: Networks that have high synchronizability tend to be dissasoratative.

Figure 6 shows how diameter, shortest average path-length, clustering, and assortativity change with synchronizability. As can be seen in this figure, synchronizability improves as diameter and shortest path-length decrease. Networks with a small diameter and short average path-lengths allow information to flow between nodes rapidly. Coupling this result with the homogeneous degree distribution suggests that not only is it important to have rapid communication between nodes, but also the flow of information needs to be balanced. Last we find that

synchronizability also increases when clustering decreases. Locally the networks appear tree-like. Another interesting result is that synchronizability increases as the network becomes more dissassortative.

5. Discussion

In this paper we have explored the fitness landscape of coupled oscillators. Our analysis reveals that as the problem scales (number of nodes increases) the fitness landscape becomes less rugged, contains more smooth regions, and the optima become easier to discover once their basin of attraction has been reached. However, the distance of the optima from random graph initial conditions grows as $O(N^4)$. With this knowledge of the structure of the fitness landscape we developed a stochastic hill-climbing routine to construct networks with optimized synchronization properties. Building an ensemble of optimized networks, we analyzed the topological properties associated with improved synchronization. We found that networks with superior synchronization properties tend to have short average path-lengths and exhibit disassortative degree mixing. A reduced cliquishness and a reduced number of small cycles makes them appear locally tree-like.

Further analyzing the characteristics of networks with superior synchronizability we find that their degree distributions have a very small variance in comparison with the initial configurations. This explains the very homogeneous load distributions (distributions of the number of shortest paths running through each node). The above result suggests that the networks explored here may belong to the class of (almost) L/N -regular graphs. Studies of random L/N -regular graphs have identified very similar properties [20]. However, a more detailed analysis shows that the optimized networks exhibit properties which are a consequence of more than the collapse of the degree variance. We note that the optimized networks are substantially smaller, more disassortative, and even less cliquish than random L/N -regular graphs. This observation allows us to conclude that a small diameter and disassortative degree mixing are features that *per se* improve network synchronizability. It is important to know how to best generate enhanced synchronization properties. From our findings, the following procedure appears to be the most practical way to construct networks with superior synchronizability. Begin by constructing an L/N -regular random graph (see [21]). Then proceed by applying the search algorithm described in section 4 until an optimal configuration is reached.

Finally, we note that many biological networks show disassortative mixing of node degrees. One example of a system where synchronization may play an important role in the dynamics is the neural network of *C. Elegans*. From our findings we can speculate that apart from enhanced stability against dynamical perturbations [22], dissassortative

mixing could also be the result of the evolution of these networks towards a topology that stabilizes synchronized states.

Acknowledgments

The authors would like to thank Hussain Abbass for a number of useful discussions about this work.

References

- [1] Albert, R. and Barabási, A.-H., “Statistical Mechanics of Complex Networks,” *Review of Modern Physics*, **74** (2002) 47–97.
- [2] Watts, D. J., *Small Worlds* (Princeton University Press, Princeton, NJ, 1999).
- [3] Strogatz, S. H., “Exploring Complex Networks,” *Nature*, **410** (2001) 268–276.
- [4] Variano, E. A., McCoy, J. H., and Lipson, H., “Networks, Dynamic and Modularity,” *Physical Review Letters*, **92**(18) (2004) 188701-1–4.
- [5] Strogatz, S. H., *Sync: How Order Emerges from Chaos in the Universe, Nature, and Daily Life* (Hyperion, New York, 2003).
- [6] Hong, H., Kim, B. J., Chio, M. Y., and Park, H., “Factors that Predict Better Synchronizability on Complex Networks,” arXiv:cond-mat/0403745v1, 2004.
- [7] T. Nishikawa, A. E. Motter, Y-C. Lai, and F. C. Hoppensteadt, “Heterogeneity in Oscillator Networks: Are Smaller Worlds Easier to Synchronize?” *Physical Review Letters*, **91**(1) (2003) 014101.
- [8] Strogatz, S. H., “From Kuramoto to Crawford: Exploring the Onset of Synchronization in Populations of Coupled Oscillators,” *Physica D*, **143** (2000) 1–20.
- [9] Winfree, A. T., *The Geometry of Biological Time* (Springer, New York, 2001).
- [10] Pecora, L. M., and Carroll, T. L., “Master Stability Functions for Synchronized Coupled Systems,” *Physical Review Letters*, **80**(10) (1998) 2109–2112.
- [11] Winfree, A. T., “Biological Rhythms and the Behavior of Populations of Coupled Oscillators,” *Journal of Theoretical Biology*, **16** (1967) 15–42.
- [12] Wright, S., “The Roles of Mutation, Inbreeding, Crossbreeding, and Selection on Evolution,” in *Proceedings of the Sixth International Conference on Genetics*, edited by D. F. Jones, Brooklyn, NY, 1932.

- [13] Teo, J. and Abbass, H. A., “An Information Theoretic Landscape Analysis of Neuro-controlled Embodied Organisms,” *Neural Computation and Applications*, **13** (2004) 80–89.
- [14] Weinberger, E., “Correlated and Uncorrelated Fitness Landscapes and How to Tell the Difference,” *Biological Cybernetics*, **63** (1990) 325–336.
- [15] Vassilev, V. K., Fogarty, T. C. and Miller, J. F., “Information Characteristics and the Structure of Landscapes,” *Evolutionary Computation*, **8**(1) (2000) 31–60.
- [16] Erdös, P. and Rényi, A., “On Random Graphs I.” *Publicationes mathematicae*, Debrecen, **6** (1959) 290–297.
- [17] Watts, D. J. and Strogatz, S. H., “Collective Dynamics of ‘Small-World’ Networks,” *Nature*, **393** (1998) 440–442.
- [18] Newman, M. E. J., “Mixing Patterns in Networks,” *Physical Review E*, **67** (2003) 026126.
- [19] Freeman, L. C., “Set of Measures of Centrality Based on Betweenness,” *Sociometry*, **40**(1) (1977) 35–41.
- [20] Brede, M. and Newth, D., “Evolving Networks with Optimized Synchronization Properties,” *Physical Review E* (under review).
- [21] Wormald, N. D., “Models of Random Regular Graphs,” in *London Mathematical Society Lecture Note Series*, edited by J. D. Lamb and D. A. Preece (Cambridge University Press, Cambridge, 1999).
- [22] Brede, M. and Sinha, S., “Assortativity Reduces Stability of Degree Correlated Networks,” (in preparation).